Eur. Phys. J. A **14**, 355–364 (2002)
DOI 10.1140/epja/i2002-10029-5

THE EUROPEAN PHYSICAL JOURNAL A

The use of coherent states in the variational treatment of proton-neutron interactions

J.G. Hirsch[1,a], P.O. Hess[1,b], and O. Civitarese[2,c]

[1] Instituto de Ciencias Nucleares, Universidad Nacional Autónoma de México, Apdo. Postal 70-543, Mexico 04510 D.F.
[2] Department of Physics, University of Plata, c.c. 67, (1900) La Plata, Argentina

Received: 19 February 2002 / Revised version: 15 April 2002
Communicated by P. Schuck

Abstract. Coherent states are used as trial states to determine, variationally, the structure of the eigenvectors belonging to a schematic Hamiltonian consisting of single-particle, pairing and residual proton-neutron interaction terms. It is shown that the standard proton-neutron quasiparticle random-phase approximation (*pn*-QRPA) is recovered, as a variational theory, by replacing quasiparticle pair creation and annihilation operators by bosons. It is also shown that an exact, algebra preserving, mapping of the Hamiltonian is needed to describe the spectrum beyond the QRPA phase transition. The role of the spurious components of the trial wave functions is discussed.

PACS. 21.60.Jz Hartree-Fock and random-phase approximations – 21.60.Fw Models based on group theory – 23.40.Hc Relation with nuclear matrix elements and nuclear structure

1 Introduction

The question about the validity and predictive power of approximate methods, like the particle-hole random-phase approximation (RPA) or the quasiparticle random-phase approximation (QRPA) and related formalisms, has been revisited in the last years. The interest in such a type of theoretical studies has been renewed, mainly, by the need to describe isospin-dependent nuclear correlations in the vicinity of transitions from the spherical to the deformed domains in isospace [1,2]. The notion of intrinsic and collective isospin degrees of freedom, in dealing with the theoretical description of nuclear double beta-decay transitions, has been reported in a number of publications (for a comprehensive list of references please see [3]). The use of schematic Hamiltonians [4–6], has been extremely fruitful in revealing the interplay between different degrees of freedom. We shall profit from the use of a schematic, albeit realistic, Hamiltonian in the present discussion to explore the basic structure of more realistic models. The extent to which the isospin symmetry is broken by the residual interactions, or equivalently, the induced isospin mixing in the ground state, has been studied from different corners. The reported studies included formal group theoretical approaches [7–10], boson expansions methods [11–14], collective models [15] and the comparison between the QRPA formalism and the bosonic and fermionic realizations of the problem [14]. The results of these studies can be compared with those obtained by using extensions of the QRPA formalism [16–19] or *ad hoc* renormalization procedures [20]. The group theoretical treatment of schematic proton-neutron interactions developed in [6,8] was re-phrased lately [21] in the language of a semiclassical analysis [22]. In order to introduce the material of the present work, we shall review some of the basic concepts related to the use of the variational principle. As is well known, the variational principle

$$\delta \frac{\langle \Psi | H | \Psi \rangle}{\langle \Psi | \Psi \rangle} = 0 \tag{1}$$

is equivalent to the Schrödinger equation and, for a many-body wave function $|\Psi\rangle$, it provides the best approximation to the exact solution in a given Hilbert space [23]. Trial wave functions of the exponential type

$$|\Phi(z)\rangle = N_0 \exp\left\{ \sum_{k<k'} z_{kk'} a_k^\dagger a_{k'}^\dagger \right\} |\Phi_0\rangle \tag{2}$$

are the most general Hartree-Fock (HF)–type of wave functions which can be introduced in fermionic representations, if the operators $a_k^\dagger$ are fermion creation operators, and the general RPA-type wave functions when these operators represent bosons [23]. In this work we shall describe the treatment of a model Hamiltonian by using

[a] e-mail: hirsch@nuclecu.unam.mx
[b] e-mail: hess@nuclecu.unam.mx
[c] e-mail: civitare@venus.fisica.unlp.edu.ar

different trial wave functions. Following the method presented in ref. [14], the ground-state wave function and the Hamiltonian are explicitly written in terms of fermionic, or bosonic, variables and the coefficients of the expansion are determined by a minimization. Once the structure of the ground state is determined, the spectrum of H is constructed by acting with pair creation, or boson, operators, on the variational ground state. In this manner, the eigenvalues and the matrix elements for transitions between eigenstates can be calculated and eventually compared with the exact results. The simplest trial wave function is the coherent state [24],

$$b\,|\alpha\rangle = \alpha|\alpha\rangle, \tag{3}$$

defined as the eigenstate of the boson annihilation operator. Another suitable trial wave function is a truncated representation of the coherent state, which does not include spurious states and preserves the symmetries of the Hamiltonian. Finally, one can define a trial wave function, the correlated ground state $|\mathrm{g.s.(QRPA)}\rangle$, which obeys

$$\Gamma|\mathrm{g.s.(QRPA)}\rangle = 0. \tag{4}$$

In (4), Γ is the Hermitian conjugate of the QRPA one-phonon creation operator $\Gamma^\dagger$. Since the structure of the eigenvalues of H, in the QRPA approach, is determined by the equation of motion

$$[H, \Gamma^\dagger] = \omega\Gamma^\dagger \ , \tag{5}$$

the QRPA ground state $|\mathrm{g.s.(QRPA)}\rangle$ is a coherent state associated with the operator Γ, with zero eigenvalue. It has been shown [25,26], that the RPA (or the QRPA) theory belongs to the class of variational theories. We will show in detail how the variational structure of the theory manifests itself when coherent states are used as trial states. As pointed out [27], in using boson realizations of the Hamiltonian, the adopted boson mapping should preserve the algebra of the original fermionic operators [14]. In the present work we have adopted the Dyson boson expansion method, as a convenient mapping [17,24,27]. Effects due to the violation of the Pauli principle, in the context of the boson expansion method, can be explored by using exponential and polynomial expansions. Following the method of [11,14], we shall introduce a complex order parameter to study the sensitivity of expectation values in the pn-QRPA, the exponential and in the Dyson boson expansion representations. We have found that the boson mapping describes correctly the phase transition. Clearly, the combined way consisting of the complete boson mapping of the Hamiltonian and the approximate one of the wave functions is a non-perturbative approach and it goes well beyond the mean-field approximation, as the exact solution does. We have organized the material of this work in the following manner. The formalism is presented in sect. 2, where the Hamiltonian and the essentials of the QRPA and of the Dyson boson mapping are introduced. In sect. 3 the different approximations used to construct the wave functions are described, and in sect. 4 the results corresponding to the matrix elements of the Hamiltonian H, calculated by using the approximations described in sect. 3, are shown. Results are presented and discussed in sect. 5. Conclusions are drawn in sect. 6.

2 The Hamiltonian

The Hamiltonian adopted for the present calculations is [1,2]

$$H = \sum_{pj} e_{pj} N_{pj} + \sum_{j} e_{nj} N_{nj} - G_p S_p^\dagger S_p - G_n S_n^\dagger S_n + 2\chi\beta^-\beta^+ - 2\kappa P^- P^+ \,. \tag{6}$$

This form of H has been used previously both in realistic and in schematic calculations [4–6,11,14]. It contains single-particle energies, monopole pairing terms and charge-exchange particle-hole and particle-particle (hole-hole) terms. The Hamiltonian (6) has been used both for the description of Fermi ($\Delta J = 0, \Delta T = \pm 1$) and Gamow-Teller ($\Delta J = 1, \Delta T = \pm 1$) excitations and the corresponding transitions [6,9]. For the sake of simplicity we proceed with the case of Fermi transitions, and the corresponding definitions are the following:

$$\begin{aligned}
N_{qj} &= \sum_m a^\dagger_{qjm} a_{qjm}, \\
S_q^\dagger &= \sum_{jm} a^\dagger_{qjm} a^\dagger_{\overline{qjm}}, \quad S_q = (S_q^\dagger)^\dagger, \quad q = p, n, \\
\beta^- &= \sum_{jm} \langle pjm|\tau^-|njm\rangle a^\dagger_{pjm} a_{njm}, \\
\beta^+ &= \beta^{-\,\dagger}, \\
P^- &= \sum_{jm} \langle pjm|\tau^-|njm\rangle a^\dagger_{pjm} a^\dagger_{\overline{njm}}, \\
P^+ &= P^{-\,\dagger}.
\end{aligned} \tag{7}$$

These operators are the number operator, the monopole pair operator and the charge-exchanging particle-hole and particle-particle operators, respectively. Proton and neutron single-particle orbits, of angular momentum j and projection m, are denoted by the index q ($q = p$ for protons and $q = n$ for neutrons) and $a^\dagger_{qjm}$ is a particle creation operator and $a^\dagger_{\overline{qjm}} = (-1)^{j-m} a^\dagger_{q\,j\,-m}$ its time reversal. We consider the one-shell limit of this Hamiltonian and pairing effects are accounted for by a quasiparticle mean field, defined separately for protons and neutrons [28]. In the BCS representation the quasiparticle proton-neutron pair operator has the form

$$A^\dagger = \left[\alpha_p^\dagger \otimes \alpha_n^\dagger\right]^{J=0}_{M=0}, \tag{8}$$

where $\alpha_q^\dagger$ (α_q) are quasiparticle creation (annihilation) operators. Keeping in the Hamiltonian only bilinear products of $A^\dagger$ and A, we arrive at the expression [6,8,14]

$$H = \epsilon\, C + \lambda_1 A^\dagger A + \lambda_2 (A^\dagger A^\dagger + AA)\,, \tag{9}$$

where the proton and neutron quasiparticle energies have been replaced by a common value ϵ. The operator C and the coupling constants λ_1 and λ_2 of eq. (9) are defined by

$$C = \sum_{m_p} \alpha^\dagger_{pm_p}\alpha_{pm_p} + \sum_{m_n} \alpha^\dagger_{nm_n}\alpha_{nm_n}\,, \tag{10}$$

$$\lambda_1 = 4\Omega\left[\chi(u_p^2v_n^2 + v_p^2u_n^2) - \kappa(u_p^2u_n^2 + v_p^2v_n^2)\right]\,, \tag{11}$$

$$\lambda_2 = 4\Omega(\chi+\kappa)u_pv_pu_nv_n\,, \tag{12}$$

where $2\Omega = (2j+1)$ is the degeneracy of the single j-shell in a standard notation [28]. The parameters χ and κ are the strengths of the particle-hole and particle-particle channels of the monopole proton-neutron interaction, and $u_{p(n)}$ and $v_{p(n)}$, are the proton (neutron) BCS occupation numbers. In the one-shell limit, the occupation numbers v_q^2 are $\frac{N_q}{2\Omega}$. The operators $A^\dagger, A$ and C satisfy the $SU(2)$ quasispin algebra [6]

$$[A, A^\dagger] = 1 - \frac{C}{2\Omega}, \qquad [C, A^\dagger] = 2A^\dagger\ . \tag{13}$$

This model is a proton-neutron realization of the Lipkin model [29]. Previous studies of this model, which are relevant for the present work, can be found in refs. [19,25,30]. In particular, we are following the notation of ref. [31].

Exact solutions

As is shown in [31], the exact solutions of (9) are obtained by diagonalizing the Hamiltonian in the basis

$$|n\rangle = (2\Omega)^{\frac{n}{2}}\sqrt{\frac{(2\Omega-n)!}{n!(2\Omega)!}}(A^\dagger)^n|\rangle\,, \tag{14}$$

where $|\rangle$ is the quasiparticle vacuum. Acting with the quasiparticle pair creation operator on this state one obtains

$$A^\dagger|n\rangle = \sqrt{\frac{(2\Omega-n)(n+1)}{2\Omega}}|n+1\rangle, \tag{15}$$

which explicitly shows that the maximum number of pairs allowed in any state is 2Ω, as dictated by the Pauli principle. The non-zero matrix elements of the Hamiltonian are of the form

$$\begin{aligned}
\langle n|H|n\rangle &= (2\epsilon+\lambda_1)\,n + \lambda_1 n\,\frac{1-n}{2\Omega},\\
\langle n+2|H|n\rangle &= \frac{\lambda_2}{2\Omega}\sqrt{(2\Omega-n)(2\Omega-n-1)(n+1)(n+2)}\,,\\
\langle n-2|H|n\rangle &= \frac{\lambda_2}{2\Omega}\sqrt{(2\Omega-n+2)(2\Omega-n+1)n(n-1)}.
\end{aligned} \tag{16}$$

Since the Hamiltonian of eq. (9) can only connect states (14) such that $\Delta n = 0, \pm 2$, its eigenfunctions can be written in terms of linear combinations of states with even (e) or odd (o) values of n (the number of quasiparticle pairs), namely:

$$|\lambda, \mathrm{e}\rangle = \sum_{n=0}^{\Omega} C^\lambda_{n,\mathrm{e}}|2n\rangle\ \ , \qquad |\lambda, \mathrm{o}\rangle = \sum_{n=0}^{\Omega-1} C^\lambda_{n,\mathrm{o}}|2n+1\rangle. \tag{17}$$

In this notation λ is the eigenvalue index, thus $|\lambda = 1, \mathrm{e}\rangle$ and $|\lambda = 1, \mathrm{o}\rangle$ are the exact ground state of the even-even and of the odd-odd nuclei, respectively.

Boson mapping

Following the discussion presented in [14], we shall introduce a boson mapping of eq. (9) which preserves the Pauli principle. The Dyson mapping [24,27] of the Hamiltonian (9) can be performed by replacing the quasiparticle-pair operators by the corresponding Dyson images

$$(A^\dagger)_{\mathrm{D}} = b^\dagger\left(1 - \frac{b^\dagger b}{2\Omega}\right),\ \ (A)_{\mathrm{D}} = b\,,\ \ (C)_{\mathrm{D}} = 2b^\dagger b\,, \tag{18}$$

where the index D refers to the Dyson mapping and proton-neutron bosons are denoted by $b^\dagger$ or b. The operators $b^\dagger$ and b are boson creation and annihilation operators which obey exact boson commutation relations. The number of proton-neutron bosons, $n_b = \langle b^\dagger b\rangle$, is restricted by the condition $n_b \leq 2\Omega$, which guarantees that spurious, non-physical, states are excluded [24,27]. The transformed Hamiltonian is given by

$$\begin{aligned}
(H)_{\mathrm{D}} = (2\epsilon+\lambda_1)b^\dagger b - \frac{\lambda_1}{2\Omega}{b^\dagger}^2b^2 + \lambda_2\left(1-\frac{1}{2\Omega}\right){b^\dagger}^2\\
-\frac{\lambda_2}{\Omega}\left(1-\frac{1}{2\Omega}\right){b^\dagger}^3 b + \frac{\lambda_2}{4\Omega^2}{b^\dagger}^4b^2 + \lambda_2 b^2\,.
\end{aligned} \tag{19}$$

While the above form of the Hamiltonian is non-Hermitian, because we have used the non-Hermitian Dyson mapping, it has the advantage of having a finite number of terms. Thus, it can be diagonalized and the exact results can be straightforwardly compared with the approximate ones. In the limit $2\Omega \to \infty$ we obtain the simplest quasiboson image [27] of the QRPA Hamiltonian

$$H_{\mathrm{QRPA}} = (2\epsilon+\lambda_1)b^\dagger b + \lambda_2({b^\dagger}^2 + b^2). \tag{20}$$

The QRPA formalism

The main assumption of the QRPA is that the one-phonon creation operator can be built as a linear combination of proton-neutron pair creation and annihilation operators acting on the correlated vacuum (4). In the present model there is only one phonon, which is written as

$$\Gamma^\dagger = \left(XA^\dagger - YA\right), \tag{21}$$

and from this assumption the usual QRPA matrix-equations [17,31]

$$\begin{pmatrix} A, & B \\ -B, & -A \end{pmatrix}\begin{pmatrix} X \\ Y \end{pmatrix} = \omega\ U\begin{pmatrix} X \\ Y \end{pmatrix}, \tag{22}$$

are obtained. The (1×1) matrices A, B, and U are defined by the expectation values

$$\begin{aligned}
A &= \langle 0|[A, H, A^\dagger]|0\rangle, \qquad B = -\langle 0|[A, H, A]|0\rangle,\\
U &= \langle 0|[A, A^\dagger]|0\rangle,
\end{aligned} \tag{23}$$

where $[A,H,A]$ is the double commutator $[A,[H,A]]$ and $|0\rangle$ is the correlated vacuum. The normalization of the excited states $\Gamma^\dagger|0\rangle$ is obtained by evaluating the vacuum expectation value of the commutator $[\Gamma,\Gamma^\dagger]$

$$\langle 0|[\Gamma,\Gamma^\dagger]|0\rangle = (X^2-Y^2)\left(1-\frac{\langle 0|C|0\rangle}{2\Omega}\right), \qquad (24)$$

where forward (X)- and backward (Y)-going QRPA amplitudes satisfy

$$X^2-Y^2=1. \qquad (25)$$

The so-called *quasiboson approximation* is consistent with the value

$$\langle 0|\Gamma\Gamma^\dagger|0\rangle = 1, \qquad (26)$$

which is valid except in the strong coupling limit. This limit involves large values of λ_2, such as $2\lambda_2 \to 2\epsilon+\lambda_1$. In this limit $X\to\infty, Y\to\infty$ and $\langle 0|C|0\rangle \to 2\Omega$, and the QRPA eigenstate cannot be normalized. The matrix elements A and B, of the eq. (22), are obtained by assuming that the correlated vacuum and the fermionic ones coincide, *i.e.*

$$\langle 0|C|0\rangle_{\rm RPA}=0, \quad A_{\rm RPA}=2\epsilon+\lambda_1, \quad B_{\rm RPA}=2\lambda_2. \qquad (27)$$

The QRPA excitation energy ω [14] is given by $\omega = [(2\epsilon+\lambda_1)^2-(2\lambda_2)^2]^{1/2}$, and it vanishes for $2\lambda_2 = 2\epsilon+\lambda_1$. Replacing this value in eq. (22), the second condition for the wave function is obtained

$$\frac{Y}{X}=\frac{\omega-A}{B}=\frac{[(2\epsilon+\lambda_1)^2-(2\lambda_2)^2]^{1/2}-2\epsilon-\lambda_1}{2\lambda_2}, \qquad (28)$$

and the ratio $|\frac{Y}{X}|$ goes to 1 as ω approaches zero.

3 Trial states

After performing the boson mapping we shall introduce trial states, which are related to coherent states [24,27]. The simplest coherent state allows for any number of bosons, without taking into account the Pauli principle. This trial state, which is a solution of eq. (3) in the one-dimensional case, is defined as

$$|\alpha_\infty\rangle = N_\infty \exp\{-\alpha b^\dagger\}|\rangle = N_\infty \sum_{l=0}^{\infty}\frac{\alpha^l}{l!}b^{\dagger l}|\rangle. \qquad (29)$$

The excited state $|1_\infty\rangle$ is

$$|1_\infty\rangle = \frac{N_{1\infty}}{N_\infty}\, b^\dagger\, |\alpha_\infty\rangle. \qquad (30)$$

Although simpler in form, these trial states have many shortcomings since they include Pauli-principle violating terms. Also, the excited state is orthogonal to the ground state only when $\alpha=0$. Both states have odd- and even-number of bosons, which are not mixed by the Hamiltonian. To overcome this problems the trial states $|\tilde\alpha\rangle$ and $\langle\alpha|$ are introduced as [14]

$$\langle\alpha| = \langle|\, N_0 \sum_{l=0}^{\Omega}\frac{\alpha^{*2l}}{(2l)!}(A)^{2l}_{\rm D} = \langle|\, N_0 \sum_{l=0}^{\Omega}\frac{\alpha^{*2l}}{(2l)!}b^{2l},$$

$$|\tilde\alpha\rangle = \tilde N_0 \sum_{l=0}^{\Omega}\frac{\alpha^{2l}}{(2l)!}(A^\dagger)^{2l}_{\rm D}|\rangle = \tilde N_0\,(2\Omega!)\sum_{l=0}^{\Omega}\left[\frac{\alpha}{2\Omega}\right]^{2l}\frac{(b^\dagger)^{2l}}{(2l)!(2\Omega-2l)!}|\rangle. \qquad (31)$$

The upper value $l=\Omega$ in the sum guarantees that the Pauli principle is observed. Since the Dyson boson mapping is non-Hermitian we have to deal with different bra ($\langle\alpha|$) and ket ($|\tilde\alpha\rangle$) spaces. The excited states are again built as a boson creation operator acting on each of these states, *i.e.*

$$\langle 1| = \tfrac{N_1}{N_0}\langle\alpha|\, b = \langle|\, N_1 \sum_{l=0}^{\Omega-1}\frac{\alpha^{*2l}}{(2l)!}b^{2l+1},$$

$$|\tilde 1\rangle = \tfrac{\tilde N_1}{\tilde N_0}\, b^\dagger|\tilde\alpha\rangle = \tilde N_1\,(2\Omega!)\sum_{l=0}^{\Omega-1}\left[\frac{\alpha}{2\Omega}\right]^{2l}\frac{(b^\dagger)^{2l+1}}{(2l)!(2\Omega-2l)!}|\rangle. \qquad (32)$$

Another type of trial wave function is the QRPA vacuum, solution of eq. (4). In the limit $2\Omega\to\infty$ the QRPA creation operator defined in eq. (21) is

$$\Gamma^\dagger = \left(XA^\dagger - YA\right) \approx \left(Xb^\dagger - Yb\right) = (b^\dagger - zb)/\sqrt{1-|z|^2}, \qquad (33)$$

where $z=Y/X$ and the normalization is fixed by (25). The QRPA vacuum $|0\rangle$ has the form

$$|0\rangle = N^0 \exp\{-z(b^\dagger)^2\}|\rangle = N^0\sum_{l=0}^{\infty}\frac{z^l}{l!}b^{\dagger 2l}|\rangle, \qquad (34)$$

and the excited state is

$$\Gamma^\dagger|0\rangle = \sqrt{1-|z|^2}\, b^\dagger|0\rangle. \qquad (35)$$

Spurious states

In realistic situations the use of the Dyson boson mapping is associated with the occurrence of spurious states, which may appear as a result of the choice of the boson basis [32]. In this context, the adequacy of the boson basis and the identification of spurious states has been discussed in [32–34]. The consequences of the use of the effective operator theory in boson mappings have been discussed in ref. [34]. The effect of spurious states caused by approximated diagonalizations and/or truncations of the basis was illustrated in ref. [34] for the cases of schematic surface delta interaction and quadrupole-quadrupole interactions. The Dyson boson mapping and related expansion techniques, require, for practical applications, the definition of a physical space, that is to say the space of bosons which are in

direct correspondence with fermion pair operators. That physical space is contained in the space of ideal bosons, and it defines the basis where the Hamiltonian can be diagonalized, at the cost of introducing spurious states. It is clear that the solutions of a fully mapped (*i.e.*, free of truncations) Hamiltonian expressed in the ideal boson space do not exhibit spurious components, but this representation is not always feasible. The consideration of solutions of the Hamiltonian in a physical boson subspace, implies the consideration, also, of spurious effects, as pointed out in [35]. In the spirit of the work of refs. [35, 36] it is shown that the results of the effective operator theory of [34] can be re-interpreted in a perturbative approach, and that this correspondence allows for the identification of spurious states. These results indicate that, as a general prescription to isolate spurious states, one can search for singularities of the similarity transformation, after performing the Dyson boson mapping.

4 Matrix elements

The expectation value of the transformed Hamiltonian, eq. (19), gives the potential-energy surface, $E(\alpha) = E_{\rm r} + iE_{\rm i}$, which depends both on the real and imaginary parts of the order parameter $\alpha = \rho e^{i\theta}$, as well as on the actual value of the coupling constants of the model [11]. The minima of this potential-energy surface can be identified by performing a variation of the order parameter for different values of χ and κ. Different regimes of the solution are determined by non-trivial values of the order parameter. In the following we have summarized the expressions needed to calculate expectation values in the different approximations, namely:

$$\langle\alpha|(b^\dagger)^{n_1}b^{n_2}|\tilde{\alpha}\rangle = N_0\tilde{N}_0(2\Omega)!\; e^{i(n_2-n_1)\theta}\; \frac{\rho^{n_1+n_2}}{(2\Omega)^{n_2}} g_{n_1n_2}(\rho), \tag{36}$$

where

$$g_{n_1n_2}(\rho) = \sum_{l^*=l_{\rm min}}^{l_{\rm max}} \left(\frac{\rho^2}{2\Omega}\right)^l \frac{1}{l!(2\Omega-l-n_2)!}\,, \tag{37}$$

with $l_{\rm max} = \min(2\Omega - n_1, 2\Omega - n_2)$, $l_{\rm min} = {\rm mod}(n_1, 2)$, and l^* indicates that the sum involves only odd or even integers starting from $l_{\rm min}$;

$$\langle 1|(b^\dagger)^{n_1}b^{n_2}|\tilde{1}\rangle = N_1\tilde{N}_1(2\Omega-1)!\; e^{i(n_2-n_1)\theta}\; f_{n_1n_2}(\rho), \tag{38}$$

where

$$f_{n_1n_2}(\rho) = \sum_{l^*=k_{\rm min}}^{l_{\rm max}} \frac{\rho^{2l+n_1+n_2-2}}{(2\Omega)^{l+n_2-1}} \frac{(l+n_1)(l+n_2)}{l!(2\Omega-l-n_2)!}\quad, \tag{39}$$

with $k_{\rm min} = 1 - {\rm mod}(n_2, 2)$, and

$$\langle\alpha_\infty|(b^\dagger)^{n_1}b^{n_2}|\alpha_\infty\rangle = \; e^{i(n_2-n_1)\theta}\; \rho^{n_1+n_2}, \tag{40}$$

$$\langle 1_\infty|(b^\dagger)^{n_1}b^{n_2}|1_\infty\rangle = e^{i(n_2-n_1)\theta}\rho^{n_1+n_2} \times \frac{(n_1n_2\rho^{-2}+n_1+n_2+1+\rho^2)}{1+\rho^2}. \tag{41}$$

For the QRPA wave function the inversion of eq. (33) [25, 26] leads to

$$\begin{aligned} b^\dagger &= (\Gamma^\dagger + z\Gamma)/\sqrt{1-|z|^2}, \\ b &= (\Gamma + z^*\Gamma^\dagger)/\sqrt{1-|z|^2}. \end{aligned} \tag{42}$$

The evaluation of the matrix elements is straightforward, giving

$$\begin{aligned} \langle 0|b^\dagger b|0\rangle &= \frac{|z|^2}{1-|z|^2}, \quad \langle 0|\Gamma b^\dagger b\Gamma^\dagger|0\rangle = \tfrac{1+|z|^2}{1-|z|^2}, \\ \langle 0|b^\dagger b^\dagger|0\rangle &= \frac{z}{1-|z|^2}, \quad \langle 0|\Gamma b^\dagger b^\dagger\Gamma^\dagger|0\rangle = \tfrac{3z}{1-|z|^2}, \\ \langle 0|bb|0\rangle &= \frac{z^*}{1-|z|^2}, \quad \langle 0|\Gamma bb\Gamma^\dagger|0\rangle = \tfrac{3z^*}{1-|z|^2}. \end{aligned} \tag{43}$$

In this way we have a complete family of trial states of different complexity, which are available to compute the expectation value of the Hamiltonian. The correspondence between the complex parameters α and z is obvious, since we can treat the ratio $\frac{Y}{X}$ as a complex parameter.

We use a variational procedure to obtain the minimum for the real part of the expectation value of the Hamiltonian. It has the form

$$\begin{aligned} \frac{\langle\alpha|H|\tilde{\alpha}\rangle}{\langle\alpha|\tilde{\alpha}\rangle} = &\left[(2\epsilon+\lambda_1)\frac{g_{11}}{g_{00}} + \frac{\lambda_2}{2\Omega}\cos(2\theta) \right. \\ &\left. \times\left(\frac{g_{02}}{g_{00}} + (2\Omega-1)\frac{g_{20}}{g_{00}}\right)\right]\frac{\rho^2}{2\Omega} \\ &-\left[\frac{\lambda_1}{2\Omega}\frac{g_{22}}{g_{00}} + 2\lambda_2\cos(2\theta)\left(1-\frac{1}{2\Omega}\right)\frac{g_{31}}{g_{00}}\right] \\ &\times\frac{\rho^4}{(2\Omega)^2} + \lambda_2\cos(2\theta)\frac{g_{42}}{g_{00}}\frac{\rho^6}{(2\Omega)^4}\,, \end{aligned} \tag{44}$$

for the ground state, and

$$\begin{aligned} \frac{\langle 1|H|\tilde{1}\rangle}{\langle 1|\tilde{1}\rangle} = &(2\epsilon+\lambda_1)\frac{f_{11}}{f_{00}} - \frac{\lambda_1}{2\Omega}\frac{f_{22}}{f_{00}} + \lambda_2\cos(2\theta) \\ &\times\left[\left(1-\frac{1}{2\Omega}\right)\frac{f_{20}}{f_{00}} + \frac{f_{02}}{f_{00}} \right. \\ &\left. -\frac{1}{\Omega}\left(1-\frac{1}{2\Omega}\right)\frac{f_{31}}{f_{00}} + \frac{1}{(2\Omega)^2}\frac{f_{42}}{f_{00}}\right], \end{aligned} \tag{45}$$

for the excited state. For the exponential trial states we obtain

$$\begin{aligned} \langle\alpha_\infty|H|\alpha_\infty\rangle = &\left[(2\epsilon+\lambda_1) + \lambda_2\cos(2\theta)\left(2-\frac{1}{2\Omega}\right)\right]\rho^2 \\ &-\left[\frac{\lambda_1}{2\Omega} + \frac{\lambda_2\cos(2\theta)}{\Omega}\left(1-\frac{1}{2\Omega}\right)\right]\rho^4 \\ &+\frac{\lambda_2\cos(2\theta)}{(2\Omega)^2}\rho^6, \end{aligned} \tag{46}$$

$$\langle 1_\infty|H|1_\infty\rangle = (2\epsilon+\lambda_1)\frac{1}{1+\rho^2} + \left[6\epsilon+\lambda_1\left(3-\frac{4}{2\Omega}\right) + 3\lambda_2\cos(2\theta)\left(2-\frac{3}{2\Omega}+\frac{1}{2\Omega^2}\right)\right]\frac{\rho^2}{1+\rho^2} + \left[2\epsilon+\lambda_1\left(1-\frac{5}{2\Omega}\right)+\lambda_2\cos(2\theta) \times\left(2-\frac{11}{2\Omega}+\frac{9}{2\Omega^2}\right)\right]\frac{\rho^4}{1+\rho^2} - \left[\frac{\lambda_1}{2\Omega}+\frac{\lambda_2\cos(2\theta)}{\Omega}\left(1-\frac{1}{2\Omega}-\frac{7}{4\Omega^2}\right)\right] \times\frac{\rho^6}{1+\rho^2}+\frac{\lambda_2\cos(2\theta)}{(2\Omega)^2}\frac{\rho^8}{1+\rho^2}. \quad (47)$$

The expectation value of the Hamiltonian (20) between purely exponential coherent states is given by [14]

$$\langle\alpha_\infty|H|\alpha_\infty\rangle = \left[(2\epsilon+\lambda_1)+2\lambda_2\cos(2\theta)\right]\rho^2\,. \quad (48)$$

This quadratic dependence on ρ shows that (20) is the harmonic approximation of the Hamiltonian (19). As is well known, this approximation is valid as long as the minimum of the effective potential is located at $\rho = 0$ but it fails in the presence of a phase transition. This expectation value can be seen as the result of the trivial substitution of the operators $A^\dagger, A$ in (9) by the complex numbers $\rho e^{i\theta}, \rho e^{-i\theta}$.

However, the expectation value of the Hamiltonian (20) shows the following interesting features:

$$\langle 0|H_{\rm QRPA}|0\rangle = (2\epsilon+\lambda_1)\frac{|z|^2}{1-|z|^2}+2\lambda_2\frac{|z|\cos\theta}{1-|z|^2}\,, \quad (49)$$

$$\langle 0|\Gamma H_{\rm QRPA}\Gamma^\dagger|0\rangle = (2\epsilon+\lambda_1)\frac{1+2|z|^2}{1-|z1^2}+2\lambda_2\frac{3|z|\cos\theta}{1-|z|^2}\,, \quad (50)$$

$$\omega(z) = \langle 0|\Gamma H_{\rm QRPA}\Gamma^\dagger|0\rangle - \langle 0|H_{\rm QRPA}|0\rangle = (2\epsilon+\lambda_1)\frac{1+|z|^2}{1-|z|^2}+4\lambda_2\frac{|z|\cos\theta}{1-|z|^2}\,. \quad (51)$$

In order to complete this section, and for later use, we show the expressions corresponding to Fermi transitions [6] between coherent states. The Dyson mapping of the operator β^- of eq. (7), written in the quasiparticle representation, reads [8]

$$\beta^- = u_p v_n (A^\dagger)_{\rm D} + v_p u_n (A)_{\rm D} = u_p v_n b^\dagger\left(1-\frac{b^\dagger b}{2\Omega}\right)+v_p u_n b\,, \quad (52)$$

and the matrix elements are written as

$$\langle 1|\beta^-|\tilde\alpha\rangle = N_1\tilde N_0(2\Omega-1)! \left(u_p v_n f_{00}(\rho)+v_p u_n\cos(2\theta)\frac{\rho^2}{2\Omega}g_{02}(\rho)\right), \quad (53)$$

$$\langle 1_\infty|\beta^-|\alpha_\infty\rangle = \frac{u_p v_n}{\sqrt{1+\rho^2}}\left(1+\rho^2-(2+\rho^2)\frac{\rho^2}{2\Omega}\right) + \frac{v_p u_n}{\sqrt{1+\rho^2}}\cos(2\theta)\rho^2, \quad (54)$$

$$\langle 0|\Gamma\beta^-|0\rangle = \frac{u_p v_n}{\sqrt{1-z^2}}\left(1-\frac{z^2}{2\Omega}\right)+\frac{v_p u_n}{\sqrt{1-z^2}}z\,, \quad (55)$$

with

$$\tilde N_0 = \left[\sum_{l=0}^{\Omega}\left(\frac{\rho}{2\Omega}\right)^{4l}\frac{1}{l!}\left(\frac{(2\Omega)!}{(2\Omega-2l)!}\right)^2\right]^{-1/2}, \qquad N_1 = \left[\sum_{l=0}^{\Omega-1}\frac{\rho^{4l}}{(2l)!}(2l+1)\right]^{-1/2}. \quad (56)$$

In (53) the operator β^- connects states with even and odd number of bosons, while in (54) the trial states contain both even and odd powers of $b^\dagger$.

5 Results and discussion

The potential-energy surface $\langle H\rangle$ was minimized as a function of the complex order parameter $\alpha = \rho e^{i\theta}$. In all the cases presented in the previous section the dependence of $\langle H\rangle$ on $\phi = 2\theta$ ($\phi = \theta$ for the QRPA) is given by

$$\langle H\rangle = \mathcal{A}(\rho)+\mathcal{B}(\rho)\cos(\phi)\,, \quad (57)$$

and by the variations

$$\frac{\partial}{\partial\phi}\langle H\rangle = -\mathcal{B}(\rho)\sin(\phi) = 0\,, \qquad \frac{\partial^2}{\partial\phi^2}\langle H\rangle = -\mathcal{B}(\rho)\cos(\phi) > 0\,. \quad (58)$$

Thus, at the minimum

$$\cos(\phi) = -1\,, \quad (59)$$

if $\mathcal{B} = 2\lambda_2 > 0$. We will use this condition in the rest of the article. It is illustrative to show how the usual QRPA results are obtained by using the variational method. To find the minimum of eq. (49) we solve

$$\frac{\partial}{\partial|z|}\langle 0|H_{\rm QRPA}|0\rangle = \left[2(2\epsilon+\lambda_1)|z|+2\lambda_2(1+|z|^2)\right]/(1-|z|^2) = 0, \quad (60)$$

which has the solutions

$$z_0 = \frac{\pm[(2\epsilon+\lambda_1)^2-(2\lambda_2)^2]^{1/2}-2\epsilon-\lambda_1}{2\lambda_2}. \quad (61)$$

This value of z_0 with the positive sign coincides with the value given in (28), which was obtained by applying the standard equation-of-motion method. By calculating the excitation energy (51) at the minimum, after some simple algebra, we get

$$\omega(z_0) = [(2\epsilon+\lambda_1)^2-(2\lambda_2)^2]^{1/2}\,, \quad (62)$$

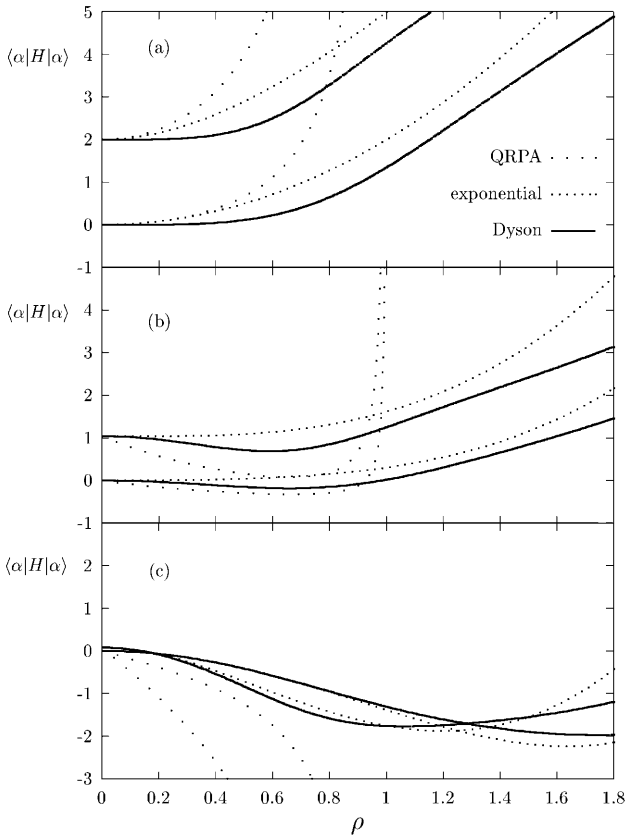

Fig. 1. Expectation values of the Hamiltonian, on the ground and excited states, as a function of the order parameter ρ. The energies are obtained by using the trial wave functions described in the text. We denote the expectation values as follows: $\langle 0|H_{\rm QRPA}|0\rangle$ and $\langle 0|\Gamma H_{\rm QRPA}\Gamma^\dagger|0\rangle$ as "QRPA", $\langle\alpha_\infty|H|\alpha_\infty\rangle$ and $\langle 1_\infty|H|1_\infty\rangle$ as "exponential", and $\langle\alpha|H|\tilde{\alpha}\rangle$ and $\langle 1|H|\tilde{1}\rangle$ as "Dyson". Panels (a), (b) and (c) show the results for $\kappa = 0.0$, 0.1 and 0.2 MeV, respectively. The results shown in (a) correspond to $\lambda_1 = \lambda_2 = 0$, for which the Hamiltonian of eq. (19), is quadratic in $b^\dagger$ and b. In each panel, the lower group of curves represent ground-state energies, while the upper ones correspond to excited-state energies.

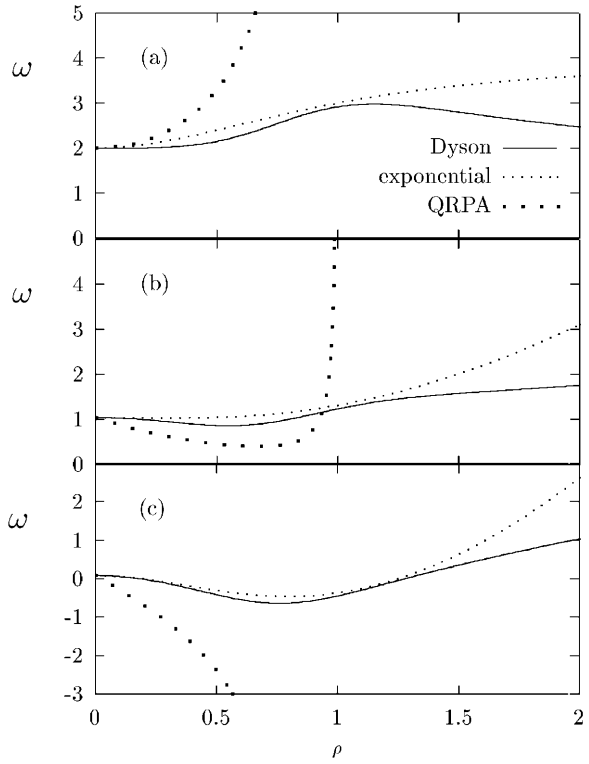

Fig. 2. Excitation energies as a function of the order parameter ρ. Panels (a), (b) and (c) show the results for $\kappa = 0$, 0.1 and 0.2 MeV, respectively.

as expected from the results of other studies [37]. In the following we shall present numerical results which correspond to the choice of the model parameters (eqs. (9) and (12)):

$$\Omega = 5\,,\quad N_p = 4\,,\quad N_n = 6\,,\quad \epsilon = 1.0\text{MeV}\,,\quad \chi = 0\,. \quad (63)$$

The quantities N_p and N_n are the number of active protons and neutrons, respectively, considered in the BCS equations. The particle-particle (proton-neutron) strength κ is varied in the range $0 \leq \kappa \leq 0.2$ MeV. Inserting these numerical values in (12) the parameters in the Hamiltonian (9) take the simple form $\lambda_1 = -9.6\kappa$, and $\lambda_2 = 4.8\kappa$. The critical behavior of the potential-energy surfaces is shown in fig. 1, where the values obtained by using the QRPA, the exponential, and the Dyson approximation, are shown. Due to its normalization the QRPA wave function cannot be evaluated beyond $|z| \to 1$, where the energies go to infinity. The Dyson approximation takes into account the Pauli principle at the level of the wave function and exhibits a saturation at $n_b = 2\Omega$, with the asymptotic value $(\rho \to \infty)$ $\langle\alpha|H|\alpha\rangle = 2\epsilon n_b$. For the three trial wave functions, the energies monotonically increase with ρ and have their minimum at $\rho = 0$. For $\kappa = 0.1$ MeV, fig. 1(b), the QRPA curve goes to infinity again, but now the change in the slope occurs closer to $|z| = 1$. The other curves are similar, but beyond $\rho \sim 2.0$ the exponential trial state has a maximum and then goes steeply to minus infinity [14] as a consequence of the violation of the Pauli principle. Excited-states energies closely follow the behavior of the ground-state energies. For the QRPA and Dyson trial states the minima in the energy are clearly seen around $\rho = 0.8$. The exponential trial state still has its minimum at $\rho = 0$, it has not yet suffered the transition to the deformed ground state. In fig. 1(c) we present the results for $\kappa = 0.2$ MeV. This value lies beyond the phase transition, which strongly modifies all the expectation values. Now, the excited state energies lie below the spherical ground-state one, as expected in a permanently deformed regime. The QRPA trial state has a maximum at $\rho = 0$. This feature is the so-called collapse of the QRPA [38], where $2\lambda_2 > 2\epsilon + \lambda_1$ and ω becomes purely imaginary. The other two curves recover the normal order around $\rho = 1.3$, where there is a crossing between the ground and excited states. Since the minimum lies in this second region, these approximations are still able to describe the physics beyond the QRPA phase transition. To clarify this last point the excitation energy, defined as the difference between the

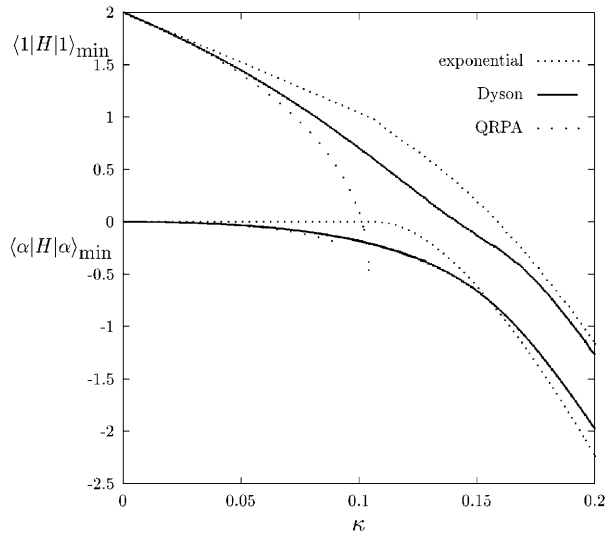

Fig. 3. Expectation value of the Hamiltonian at the minimum for the ground and excited trial states as a function of κ.

expectation values of the Hamiltonian evaluated in the excited and ground state, respectively, is plotted in fig. 2 for the three trial states. The values are displayed by using the same conventions of fig. 1. For $\kappa = 0$, panel (a), it is seen that the excitation energies also have a minimum at $\rho = 0$, which is displaced to $\rho \approx 0.8$ for $\kappa = 0.1$ MeV, panel (b), except for the exponential wave function. For $\kappa = 0.2$ MeV, panel (c), the three excitation energies are negative up to $\rho \approx 1.3$. From that point on they are positive for the Dyson and exponential trial wave functions. The previous results describe intrinsic properties of the expectation values, but the observable energies are those which minimize them. The expectation values of the Hamiltonian at the minimum are presented in fig. 3, for the considered three trial wave functions, and as a function of the interaction strength κ. The lower curves represent the ground-state energies and the upper curves the excited states ones. The QRPA energies go to minus infinity for values of κ slightly larger than 0.1 MeV. The Dyson and exponential trial states show a similar behavior. However, while the Dyson trial states become more bound, the exponential trial states are sensitive to the presence of the residual interaction for $\kappa > 0.1$ MeV. There, a sudden phase transition takes place, showing the influence of spurious components in the trial wave function [14,23]. The decrease of the energy of the exponential excited state reflects the change in λ_1 as a function of κ without any residual effect related to λ_2. Figure 4 depicts the behavior of the excitation energy as a function of κ. In this figure we have included the results for the three different trial wave functions and the exact one for comparison. The QRPA collapse at $\kappa \approx 0.1$ MeV is clearly shown. The exponential trial states overestimates the excitation energy, while the results obtained with the Dyson wave function are very close to the exact results up to $\kappa \approx 0.12$ MeV. In fig. 5 the number of bosons (or quasiparticle pairs) in the ground states (a) and excited states (b) are shown as functions of κ. This number is a measure of the ground-state correlations and it diverges when the QRPA approaches the point of collapse. The exponential wave functions show the phase transition again, as the sudden increase in the number of bosons around $\kappa = 0.1$ MeV. The Dyson trial wave function reproduces fairly well the number of bosons in the ground state, but largely overestimates its number in the excited state. Finally, fig. 6 shows results for transitions induced by the Fermi β^--operator (cf. eq. (52)).

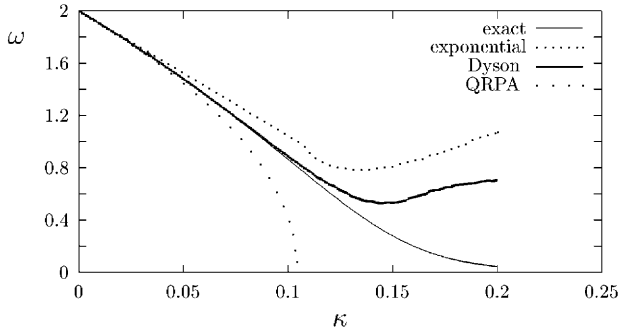

Fig. 4. Excitation energies as a function of κ.

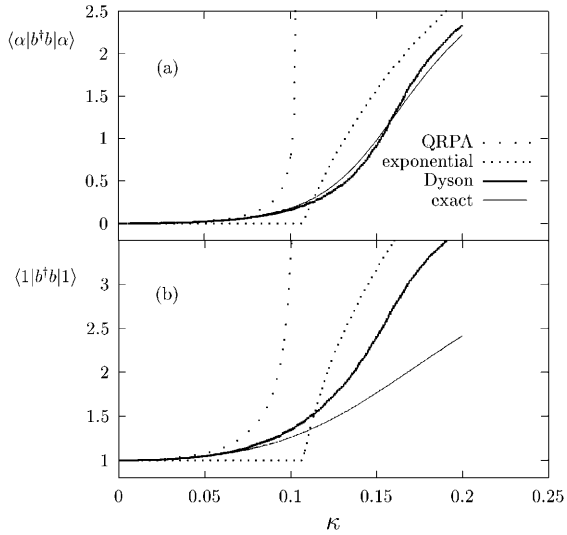

Fig. 5. The expectation value of the number of proton-neutron pairs as a function of κ for the ground (a) and excited (b) trial wave functions.

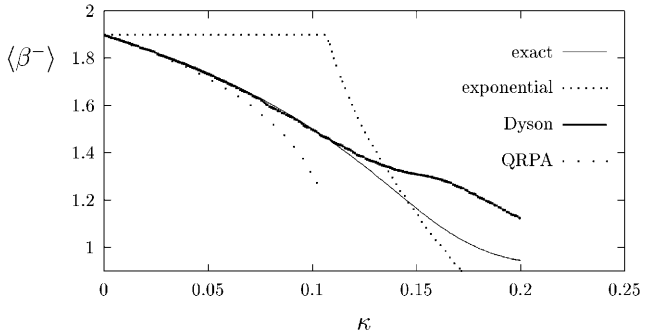

Fig. 6. The Fermi beta-transition amplitudes as a function of κ.

The results are presented as a function of κ and, as in the previous figure, they include the three different trial wave functions and the exact results. In general the transition amplitudes decrease as the residual interaction increases. However, the exponential trial states only show this effect after the phase transition, *i.e.* away from the point where the QRPA collapses. The Dyson states are again very close to the exact transition amplitudes up to $\kappa \approx 0.12$ MeV.

6 Conclusions

In the present work we have described the results of the combined application of the Dyson boson mapping technique and of the use of a coherent-state representation to characterize phase transitions. We have applied this method to study the phase domains of a schematic Hamiltonian, involving correlations in the ground state and in excited states. For the considered example we have shown that the usual QRPA approach can be obtained as the result of a variational calculation. The proof involves the use of the bosonic image of the Hamiltonian and a trial state which is the coherent state associated to the QRPA boson operator. In more complex situations, with more than one degree of freedom, one cannot extract an exact QRPA vacuum state. It can be defined only if the quasi-boson approximation is adopted to calculate expectation values and commutators. In this general case the QRPA theory loses its variational interpretation [26].

Exponential trial states, which are coherent states in the traditional sense, exhibit a sudden phase transition from the boson vacuum to a correlated ground state. The sudden effect is related with the violation of the Pauli principle and with the presence of spurious mixing of odd and even number of bosons in the wave functions. The Dyson trial states are built as finite sums and they do not contain spurious states. The excitation energies, number of bosons and beta-transition amplitudes evaluated using the Dyson trial states are very close to the exact values. These results are relevant in the context of the coherent-state description of systems based on the $SO(5)$ and $SO(8)$ algebras [6,7]. In these cases, no problems with spurious states occur because there is an exact decoupling of the collective space to the one of the spurious states [10,39]. Spurious states appear in the $SO(5)$ and the $SO(8)$ models when the number of bosons is larger than (2Ω) [39]. In the more general situations, if the symmetries of the Hamiltonian are preserved by the boson mapping, the ideal basis can be labeled by the quantum numbers of the symmetry operators, and spurious states can approximately be removed by performing variations around values fixed by the symmetry. This is the procedure which we have adopted in the present work.

This work was supported in part by CONACyT, and by a CONACyT-CONICET agreement under the project *Algebraic methods in nuclear and subnuclear physics*. O. Civitarese is a fellow of the CONICET, Argentina.

References

1. P. Vogel, M.R. Zirnbauer, Phys. Rev. Lett. **57**, 3148 (1986).
2. O. Civitarese, A. Faessler, T. Tomoda, Phys. Lett. B **194**, 11 (1987).
3. J. Suhonen, O. Civitarese, Phys. Rep. **300**, 124 (1998).
4. V.A. Kuz'min, V.G. Soloviev, Nucl. Phys. A **486**, 118 (1988).
5. O. Civitarese, J. Suhonen, Nucl. Phys. A **578**, 62 (1994).
6. J.G. Hirsch, P.O. Hess, O. Civitarese, Phys. Rev. C **54**, 1976 (1996).
7. J. Engel, P. Vogel, M.R. Zirnbauer, Phys. Rev. C **37**, 731 (1988).
8. J.G. Hirsch, P.O. Hess, O. Civitarese, Phys. Lett. B **390**, 36 (1997); Phys. Rev. C **56**, 199 (1997); Rev. Mex. Fis. **43**, S1 78 (1997).
9. J. Engel, S. Pittel, M. Stoitsov, P. Vogel, J. Dukelsky, Phys. Rev. C **55**, 1781 (1997).
10. J. Dobes, S. Pittel, Phys. Rev. C **57**, 688 (1998).
11. O. Civitarese, P.O. Hess, J.G. Hirsch, Phys. Lett. B **412**, 1 (1997).
12. M. Sambataro, J. Suhonen, Phys. Rev. **56**, 782 (1997).
13. M. Sambataro, Phys. Rev. **59**, 2956 (1999).
14. J.G. Hirsch, P.O. Hess, O. Civitarese, Phys. Rev. C **60**, 064303 (1999).
15. D.R. Bes, J. Kurchan, *The Treatment of Collective Coordinates in Mechanical Systems; an Application to the BRST Invariance*, Lect. Notes Phys., Vol. **34** (World Scientific, Singapore, 1990); D.R. Bes, O. Civitarese, N.N. Scoccola, Phys. Lett. B **446**, 93 (1999).
16. K. Hara, Progr. Theor. Phys. **32**, 88 (1964).
17. D.J. Rowe, Phys. Rev. **175**, 1283 (1968); Rev. Mod. Phys. **40**, 153 (1968); *Nuclear Collective Motion* (Methuen, Co. Ltd., London, 1970).
18. F. Catara, N. Dinh Dang, M. Sambataro, Nucl. Phys. A **579**, 1 (1994).
19. P. Schuck, S. Ethofer, Nucl. Phys. A **212**, 269 (1973).
20. J. Toivanen, J. Suhonen, Phys. Rev. Lett. **75**, 410 (1995).
21. F. Simkovic, A.A. Raduta, M. Veselsky, Amand Faessler, Phys. Rev. C **61**, 044319 (2000).
22. A.A. Raduta, O. Haug, F. Simkovic, Amand Faessler, J. Phys. G: Nucl. Part. Phys. **26**, 1327 (2000).
23. P. Ring, P. Schuck, *The Nuclear Many-Body Problem* (Springer-Verlag, New York, 1980).
24. K.T. Hecht, *Vector Coherent State Method and its Application to Problems of Higher Symmetries*, Lect. Notes Phys. (Springer-Verlag, Heidelberg, 1987).
25. J. Dukelsky, P. Schuck, Nucl. Phys. A **512**, 466 (1990).
26. D. Janssen, P. Schuck, Z. Phys. A **339**, 43 (1991).
27. A. Klein, E.R. Marshalek, Rev. Mod. Phys. **63**, 375 (1991).
28. A. Bohr, B.R. Mottelson, *Nuclear Structure*, Vol. **II** (Benjamin, Reading, Mass., 1975).
29. H.J. Lipkin, N. Meschkov, S. Glick, Nucl. Phys. A **62**, 118 (1965).
30. O. Civitarese, M. Reboiro, Phys. Rev. C **57**, 3062 (1998).
31. J.G. Hirsch, O. Civitarese, M. Reboiro, Phys. Rev. C **60**, 024309 (1999).
32. H.B. Geyer, C.A. Engelbrecht, F.J.W. Hahne, Phys. Rev. C **33**, 1041 (1986).
33. Dobaczewski, H.B. Geyer, F.W. Hahne, Phys. Rev. C **44**, 1030 (1991); J. Dobaczewski, Nucl. Phys. A **369**, 213; 237 (1981); **380**, 1 (1982).
34. P. Navratil, H. Geyer, Nucl. Phys. A **556**, 165 (1993).

35. P. Park, Phys. Rev. C **35**, 807 (1987).
36. O. Civitarese, H. Geyer, M. Reboiro, submitted to Phys. Rev. C.
37. J. Dukelsky, J.G. Hirsch, P. Schuck, Eur. Phys. J. A **7**, 155 (2000).
38. O. Civitarese, A. Faessler, J. Suhonen, X.R. Wu, J. Phys. G: Nucl. Part. Phys. **17**, 943 (1991).
39. O. Civitarese, P.O. Hess, J.G. Hirsch, M. Reboiro, Phys. Rev. C **61**, 064303 (2000).